Mechanical Systems and Signal Processing 231 (2025) 112674

Contents lists available at ScienceDirect

Mechanical Systems and Signal Processing

journal homepage: www.elsevier.com/locate/ymssp

Full Length Article

Novel two-stage adaptive weight coefficients for Finite Element Model Updating of a cable-stayed bridge via sensitivity analysis and Kriging model

Shiqiang Qin [a], Jialong Huang [a], Shiwei Li [b,c], Yunlai Zhou [d,*], Magd Abdel Wahab [e,f,g,*]

[a] School of Civil Engineering and Architecture, Wuhan University of Technology, Wuhan 430070 Hubei, China
[b] China Railway Siyuan Survey and Design Group Co., Ltd., Wuhan 430063 Hubei, China
[c] China Railway 23rd Bureau Group Co., Ltd., Chengdu 610072 Sichuan, China
[d] State Key Laboratory for Strength and Vibration of Mechanical Structures, School of Aerospace Engineering, Xi'an Jiaotong University, China
[e] Laboratory Soete, Faculty of Engineering and Architecture, Ghent University, Technologiepark Zwijnaarde 46, Zwijnaarde B-9052, Belgium
[f] College of Engineering, Yuan Ze University, Taiwan, China
[g] Parallel and Distributed Systems Laboratory, Jožef Stefan Institute, Jamova cesta 39, SI-1000 Ljubljana, Slovenia

A R T I C L E I N F O

Communicated by Javad Baqersad

Keywords:
Finite Element Model Updating
Weight coefficient
Equal weight
Adaptive weight
Relative error
Cable-stayed bridge

A B S T R A C T

The weight coefficients of the structural response residuals in an objective function are the key parameters affecting a Finite Element Model Updating (FEMU) results. Traditional equal weight methods cannot measure the importance and relative errors of different response residuals, resulting in low prediction accuracy of the updated Finite Element (FE) model. This study proposes a two-stage adaptive weight coefficient method according to the relative errors of the measured static displacements and modal frequencies. In the first stage, high weights are assigned to low-order frequencies and large displacements because they have higher accuracy and are less affected by environmental noises than high-order frequencies and small displacements. In the second stage, the weights for the responses with small relative errors are adaptively increased to reduce the prediction errors. This approach was comprehensively validated by numerical simulations of a damaged truss under various noise conditions and a full-scale cable-stayed bridge based on experimental measurements. Results indicate that the two-stage adaptive weight coefficients improve model updating accuracy and maintains robustness under various noise conditions compared to equal weight method. The updated FE model obtained from adaptive weight method for the cable-stayed bridge shows higher accuracy in predicting frequency and displacement than that obtained from equal weight method. After the model update, the maximum relative frequency error is reduced from −16.98% to −6.18%, and that of displacement is reduced from 17.85% to 5.87%. The two-stage adaptive weight coefficients improve the accuracy of FE model updating for bridge structures.

* Corresponding authors at: Laboratory Soete, Faculty of Engineering and Architecture, Ghent University, Technologiepark Zwijnaarde 46, Zwijnaarde B-9052, Belgium (M. Abdel Wahab).
E-mail addresses: yunlai.zhou@xjtu.edu.cn (Y. Zhou), magd.abdelwahab@ugent.be (M. Abdel Wahab).

https://doi.org/10.1016/j.ymssp.2025.112674
Received 24 November 2024; Received in revised form 15 February 2025; Accepted 29 March 2025
Available online 8 April 2025

1. Introduction

FE models are extensively applied in structural safety monitoring, condition assessment, service life prediction, and the development of optimal maintenance strategies [1–3]. However, the initial FE model derived from design documents is often inaccurate in reflecting the actual conditions of a bridge [4,5]. For example, Zhu et al. constructed a multi-scale 3D FE model for a long-span bridge. They found that the main beam's displacement calculated by the FE model was about 15 % larger than that obtained from the experimental measurement under the same conditions [6]. Gou et al. constructed a FE model of a cable-stayed bridge using design drawings. The relative errors between the experimental and calculated first ten frequencies reached −17.6 % [7]. Luo et al. found a relative error of 17.34 % for the first-order frequency and a significant deviation between measured and calculated static displacements when comparing actual structure data with the initial FE model [8]. Therefore, FE model updating, which seeks to diminish the discrepancy between experimentally measured and calculated values by adjusting the structural parameters, has attracted increasing attention [9]. Ereiz et al. conducted a comprehensive review of FEMU [10].

Currently, sensitivity-based FEMU has become the predominant technique for bridges. In recent years, Deep Neural Network (DNN) have shown potential in solving forward and inverse problems in FE optimization, offering a novel and valuable approach for model updating [11,12]. However, the application of this method in large bridge engineering optimization is still in the exploratory stage, mainly limited by computational cost and physical interpretability, with the engineering reliability remaining unclear. Therefore, the progress of current FE model updating still largely relies on in-depth research on mainstream approach. This approach defines an objective function by utilizing the residuals of static and dynamic responses. The objective function's minimum can be determined by various optimization algorithms through the iterative updating of design parameters that are sensitive to structural damages. For complex structures, surrogate models like the Kriging model, response surface, and Gaussian process can be employed to save computational cost. A key challenge in FEMU is the construction of a reasonable objective function. Objective functions are mainly divided into single-objective and multi-objective functions. Multi-objective functions define multiple optimization targets for different residuals and do not require weight coefficients [13,14]. The Pareto frontier solutions of multi-objective functions are obtained through multi-objective optimization algorithms, which could be very time-consuming. Additionally, balancing the importance of multiple objectives and making the best decision among conflicting solutions remains challenging. In engineering optimization, single-objective functions are more commonly used than multi-objective functions due to their straightforward concept and ease of implementation. A single-objective function may combine different objectives into one objective function by using the weighted sum method [15,16], constraint method [17,18], and equality constraint method [19]. Among them, the weighted sum method has high computational efficiency and owns a unique solution, making it widely used. However, reasonably determining the weight coefficients remains challenging [20–22]. Some studies determine weight coefficients through trial and error [23] and statistical criteria [24]. However, these methods lack general applicability and significantly increase the computational burden. Therefore, the equal weight and empirical weight methods are widely used in engineering practice [25]. Cismaşiu et al. constructed an equal weight objective function based on natural frequencies and mode assurance criterion and successfully updated a pedestrian bridge [26]. Although the equal weight objective function is easy to implement, it cannot measure the relative importance of different responses. Li et al. constructed an objective function using mode shapes and frequencies, and formulated weight coefficients based on the relative importance of each mode [27]. They found that the updated frequencies have higher accuracy than the equal weight objective function through the model updating of an offshore platform structure. Deng et al. combined frequencies and strains to construct an objective function. They determined weight coefficients based on response sensitivity and importance, ensuring that the relative importance of each residual term was addressed [28]. He et al. assigned higher weights to mode shapes due to their high sensitivity to structural stiffness changes. They updated the model of a small-span skewed highway bridge [29]. Eskew et al. used the coordinate modal assurance criterion and natural frequencies to construct the objective function for updating a five-story frame model [30]. They found that noise affected mode shapes about ten times more than frequencies and set a weight coefficient ratio of 10:1 between mode shapes and frequencies. Ye et al. developed objective functions using mode shapes, frequencies, strains, and displacements. They assigned different weight coefficients to different responses for updating a multi-beam steel truss bridge's FE model [31]. The weight coefficients of the objective function were assigned based on the authors' engineering judgment and, therefore, lacked general applicability. Additionally, some scholars developed new updating indices to avoid the difficulty of setting weight coefficients in single-objective functions. For example, modal flexibility is the combined contribution of all natural frequencies and their corresponding mode shapes. It can construct objective functions without considering the weights of individual modes [32,33]. Qin et al. introduced the displacement assurance criterion to establish an objective function and successfully updated a cable-stayed bridge without relying on weight coefficients [34,35]. However, constructing a new index requires strict requirements for experimental measurements. In a nutshell, there is currently a lack of an effective method for defining the weight coefficients of residual functions in FEMU. In order to solve this issue, this study proposes two-stage adaptive weight coefficients that assign the weights based on the relative errors of the experimental measurements. For modal frequency, the lower-order modes of a bridge are easily excited by ambient excitation and less affected by environmental noise, resulting in high testing accuracy [1]. For static displacements, each static load case has specific load arrangements. Under these loads, only the measurement points with large displacements are critical for assessing the bridge's overall stiffness and ultimate bearing capacity. Additionally, data from large displacement points are relatively stable and less affected by measurement equipment and environmental factors [24]. Based on the abovementioned fact, the first stage of the proposed two-stage adaptive weight coefficients assigns high weights to low-order frequencies and large values of displacements. Note that the abovementioned knowledge about accuracy is a general rule, and measurements, which do not conform to this rule, exist. Nevertheless, the responses with small relative errors generally have high credibility. Therefore, in the second stage, the weight coefficients are adaptively adjusted during iterations, and high weights are assigned to those responses with small relative errors. A FEMU framework is introduced using the proposed two-stage weight coefficients, Kriging surrogate model, and Particle Swarm Optimization (PSO). The Kriging surrogate model is employed to evaluate the objective function during iteration and thus save computational cost. The PSO is employed to identify the optimal solution of the objective function within its design space.

This paper is structured as follows. Section 2 briefly presents the theoretical foundation of FEMU, including the definitions of model updating and objective functions, as well as the fundamental theories of the Kriging model and the PSO algorithm. Section 3 introduces the two-stage adaptive weight coefficients and the FEMU framework. Section 4 numerically updates a damaged simply supported truss under various noise conditions to test the performance of the adaptive weight coefficients. Section 5 updates the FE model of a cable-stayed bridge using measured frequencies and displacements. The results obtained from the two-stage adaptive weight coefficients and equal weight method are compared and discussed. Finally, conclusions are drawn .

2. Theory formulations of FEMU

2.1. Definition of the objective function

The objective function quantifies the discrepancy between the measured and calculated responses [36]. It can be composed of different types of structural response residual functions, where the weight coefficients measure the relative importance of different responses. Therefore, the objective function $F(\boldsymbol{\theta})$ can be expressed by:

$$minF(\theta) = \sum\nolimits_{\lambda=1}^{p} \omega_\lambda r_\lambda(\theta)$$

$$s.t.\ \theta_s^{min} \le \theta_s \le \theta_s^{max} \tag{1}$$

where $\boldsymbol{\theta}_s^{\min}$ and $\boldsymbol{\theta}_s^{\max}$ represent the limits of the s-th design parameter. P denotes the number of structural responses, ω_λ represents the weight coefficient for the λ-th structural response component, $\boldsymbol{\theta}$ denotes the vector of parameters to update and $r_\lambda(\boldsymbol{\theta})$ represents the residual function of the λ-th structural response. In this work, the objective function is defined using the modal frequency residual and displacement residual functions. To ensure the robustness of the FEMU, when using frequency as the objective for the update, the computed modes of the FE model before and after updating must correspond correctly with the experimental modes, ensuring that the sequence of frequencies of the FE model is consistent with the actual structure. To achieve this, the Modal Assurance Criterion (MAC) is used to quantify the degree of modal matching [37]. When the MAC value between the computed and experimental modes is close to 1.0 (typically greater than 0.9), they are considered to represent the same mode. To avoid the influence of different responses' dimensions, the dimensionless relative error is used to define the response residual function. Specifically, the residual function can be expressed as:

$$r_\lambda(\boldsymbol{\theta}) = \left(\frac{U_{\mathrm{cal},\lambda} - U_{\mathrm{exp},\lambda}}{U_{\mathrm{exp},\lambda}}\right)^2 \tag{2}$$

where $U_{\mathrm{exp},\lambda}$ and $U_{\mathrm{cal},\lambda}$ denote the measured and calculated values of the λ-th response, respectively.

2.2. Kriging surrogate model

For sensitivity-based FEMU, iterative updates of the objective function require multiple calls of the FE model for response calculations, resulting in a substantial computational burden. Surrogate models can effectively capture the implicit relationships between parameters and responses [38,39], thereby replacing the complex FE model for evaluating the objective function and improving computational efficiency [34]. The Kriging model provides linear, unbiased, minimum variance estimates of unknown features in a region based on several information samples, achieving high-accuracy predictions with only a few samples [40]. It comprises two components: linear regression and random distribution. Given w, q-dimensional sample points inputs $\boldsymbol{X} = \{\boldsymbol{x}_1, \boldsymbol{x}_2, \cdots, \boldsymbol{x}_w\}^T (\boldsymbol{X} \in R^{w\times q})$ and corresponding response outputs $\boldsymbol{Y} = \{y_1, y_2, \cdots, y_w\}^T (\boldsymbol{Y} \in R^{w\times 1})$, the Kriging model can be defined by:

$$y(\boldsymbol{x}_i) = \sum_{j=1}^{u} \gamma_j f_j(\boldsymbol{x}_i) + z(\boldsymbol{x}_i)(i = 1, 2, \cdots, w) \tag{3}$$

where $\sum_{j=1}^{u} \gamma_j f_j(\boldsymbol{x}_i)$ is the linear regression component, which simulates a global approximation using u polynomials. γ_j represents the regression coefficients, $z(\boldsymbol{x}_i)$ is a stochastic process that follows a normal distribution $N(0, \sigma^2)$ and performs local approximations.

The approximation performance of $z(\boldsymbol{x}_i)$ depends on the selected correlation model. Common correlation functions include exponential, linear, spline, and Gaussian functions. Among them, the Gaussian function is widely used in Kriging modeling due to its superior ability to capture nonlinear relationships between high-dimensional input variables, providing smooth approximations while ensuring computational stability. Considering the high-dimensional characteristics and computational requirements of the bridge FE model, this study chooses the Gaussian correlation function to balance approximation accuracy and computational efficiency. The reference provides a detailed theoretical derivation of the Kriging model [41].

2.3. Optimization algorithm

As mentioned in Section 2.1, model updating is fundamentally a mathematical optimization problem, where optimization algorithms are used to minimize the objective function in Eq. (1) under certain constraints, and determine the optimal parameters within the design space. The PSO is an effective population-based optimization algorithm [42]. As an excellent *meta*-heuristic algorithm, PSO can solve continuous and discrete problems, finding approximate optimal solutions in a relatively short computational time.

PSO randomly generates a group of particles and iteratively adjusts parameters to find their optimal positions. During each iteration, particles update positions and velocities by considering their own best solution P_i and the global best solution P_g. Assuming the particle swarm contains N particles in a d-dimensional objective search space, the velocity and position of the i-th particle at time step $t + 1$ are updated based on its velocity and position at time step t, as expressed by:

$$V_i^d(t+1) = \eta V_i^d(t) + c_1 k_1 [P_i^d(t) - D_i^d(t)] + c_2 k_2 [P_g^d(t) - D_i^d(t)] \tag{4}$$

$$D_i^d(t+1) = D_i^d(t) + V_i^d(t+1) \tag{5}$$

where $V_i^d(t)$ and $D_i^d(t)$ denote the velocity and position of the i-th particle, respectively, $P_i^d(t)$ represents the historical best position of the i-th particle, $P_g^d(t)$ represents the global best position; η denotes the inertia weight factor; k_1 and k_2 are random values between [0,1] and c_1 and c_2 denote the individual and social learning factors, respectively.

In the algorithmic framework of this study, the maximum number of iterations is used as the stopping criterion. Preliminary runs with multiple iteration sets are conducted, and the convergence trend of the iteration curves is analyzed to ensure that the algorithm converges before reaching the maximum number of iterations. The rate of change in the objective function value is used as the convergence criterion, with a threshold set at $\varepsilon = 1 \times 10^{-5}$. Under this premise, the optimal iteration count is determined by balancing computational cost and the rate of error reduction, ensuring a trade-off between computational efficiency and optimization accuracy. Furthermore, the stable iteration phase after convergence helps verify the robustness of the optimization results, reducing the risk of getting trapped in a local optimum due to premature termination.

2.4. The proposed two-stage adaptive weight coefficients

This section illustrates the proposed two-stage adaptive weight coefficients. A typical single-objective function-based FEMU with weight coefficients can be expressed by:

$$F = \sum_{i=1}^{m} \alpha_i \left(\frac{f_{ai} - f_{ei}}{f_{ei}} \right)^2 + \sum_{j=1}^{n} \beta_j \left(\frac{d_{aj} - d_{ej}}{d_{ej}} \right)^2 \tag{6}$$

where α_i and β_j are the weight coefficients of the i-th frequency residual and j-th displacement residual, respectively. f_{ai} and f_{ei} represent the calculated and experimental values of the i-th frequency, respectively, d_{aj} and d_{ej} represent the calculated and experimental displacement values at the j-th measurement point, respectively, m is the modal number, and n is the number of displacement measurement points.

The current model updating methods have certain limitations, particularly in terms of accuracy, as they heavily rely on the quality of bridge static and dynamic test data. If there are systematic errors in the test measurements that fail to accurately capture the actual structural response, the updated FE model may not accurately represent the real structure. Therefore, a key challenge in improving model updating accuracy lies in the reasonable determination of weight coefficients while considering the relative errors in experimental data. Because determining the weight coefficients is challenging, equal weighting is commonly used in many case studies. In the equal weight objective function, all weight coefficients are equal to 1. However, it cannot consider the relative importance of different natureal frequencies and displacements of measurement points, resulting in low accuracy of the updated FE model. As mentioned in the introduction, the bridge's dynamic and static measurements have certain reference significance for structural mechanical behavior and evaluation. Additionally, measurement errors are prevalent due to the influence of measurement equipment and environmental noise [43,44]. Therefore, this study assumes that the experimental data have different levels of credibility, and different structural responses contain varying degrees of noise. Our goal is to use the key responses with lower noise levels to guide the updating process, thereby improving the robustness of the model updating. Based on this idea, this paper proposes a two-stage adaptive weight coefficient.

In the first stage, higher weights are assigned to low-order frequencies and large displacements because they have higher accuracy and importance compared to the rest of the frequencies and displacements. Specifically, the weight coefficients of low-order frequencies and large displacements are defined according to their modal number and displacement amplitude, respectively, as expressed by:

$$\alpha_{i1} = \frac{1/f_{ei}}{\sum_{i=1}^{m} 1/f_{ei}} \tag{7}$$

$$\beta_{j1} = \frac{d_{ej}}{\sum_{j=1}^{n} d_{ej}} \tag{8}$$

where α_{i1} and β_{j1} represent the weight coefficients in the first stage. It can be concluded from Eqs. (7) and (8) that the lower the modal number, the higher the weight of the frequency, and the larger the displacement amplitude, the higher the weight of the displacement. Ideally, the updated FE model obtained from the first stage has good prediction accuracy in low-order frequency and large displacements. However, the prediction accuracy of the remaining frequencies and displacement can be further improved.

The second stage aims to improve further the FE model's prediction accuracy obtained from the first stage. At this stage, the weight coefficients are adaptively adjusted based on the relative errors of structural responses. The smaller the structural response relative errors, the higher the credibility of the measured response and, therefore, the higher the weights. The relative errors between the calculated and measured responses during each iteration can be evaluated by:

$$E_i^f = \left|\frac{f_{ai} - f_{ei}}{f_{ei}}\right|, E^f = \sum_{i=1}^{m}\left|\frac{f_{ai} - f_{ei}}{f_{ei}}\right| \tag{9}$$

$$E_j^d = \left|\frac{d_{aj} - d_{ej}}{d_{ej}}\right|, E^d = \sum_{j=1}^{n}\left|\frac{d_{aj} - d_{ej}}{d_{ej}}\right| \tag{10}$$

where E_i^f and E_j^d denote the absolute values of the relative error between the calculated and measured values of the i-th frequency and the j-th displacement during the iteration process. E^f and E^d denote the sum of the absolute value of the relative errors between the calculated and measured values of all frequencies and all displacements. The weight coefficients α_{i2} and β_{j2} in the second stage are adaptively adjusted by:

$$\alpha_{i2} = \alpha_{i1}\cdot\left(1 - \frac{E_i^f}{E^f}\right)^2/\varphi, \beta_{j2} = \beta_{j1}\cdot\left(1 - \frac{E_j^d}{E^d}\right)^2/\psi \tag{11}$$

where φ and ψ maintain a constant total weight for each iteration and can be expressed by:

$$\varphi = \sum_{i=1}^{m}\alpha_{i1}\cdot\left(1 - \frac{E_i^f}{E^f}\right)^2, \psi = \sum_{j=1}^{n}\beta_{j1}\cdot\left(1 - \frac{E_j^d}{E^d}\right)^2 \tag{12}$$

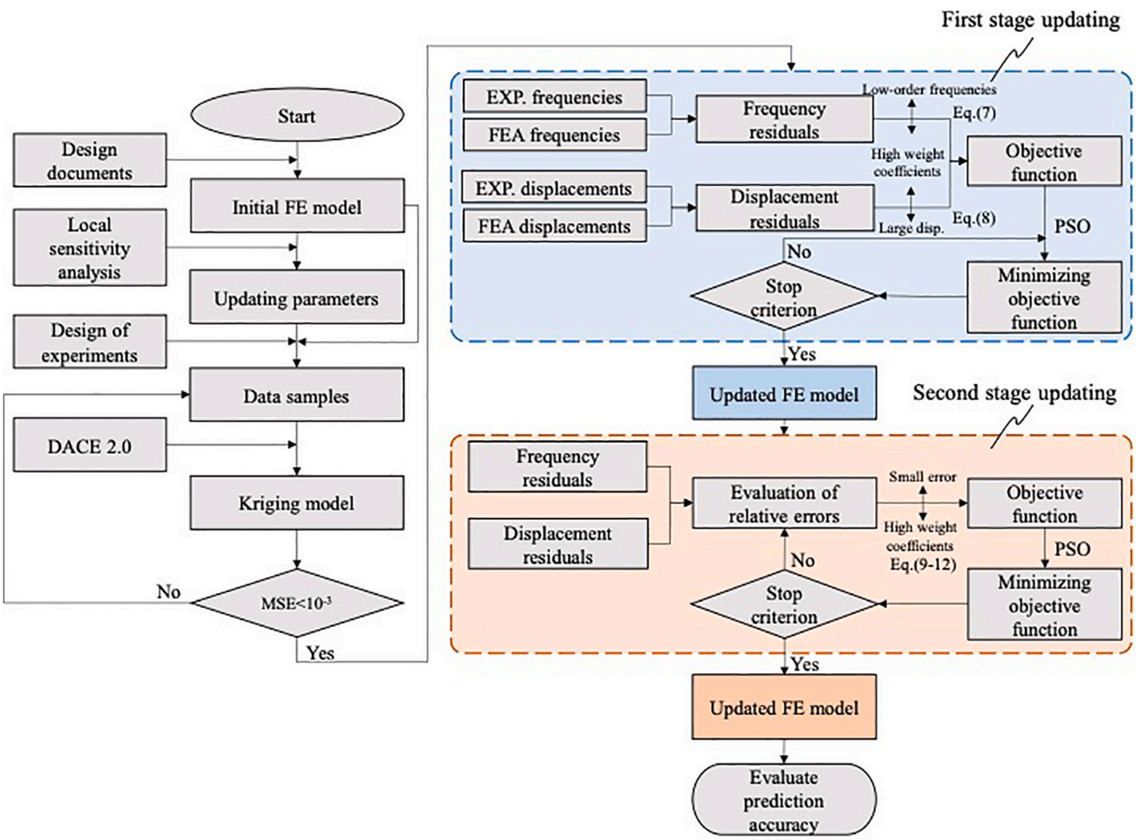

Fig. 1. Flow chart of FEMU based on two-stage adaptive weight coefficients.

The two-stage adaptive weight coefficients updating framework proposed in this study introduces an innovative improvement in model updating strategy. It incorporates a data-driven adaptive weight definition method based on experimental data, overcoming the subjectivity inherent in traditional methods that rely on experience to set weight coefficients. Additionally, the framework adopts a two-stage weighting mechanism, dynamically optimizing weight distribution during the iteration process, which enhances the stability and reliability of the model updating. Furthermore, the framework exhibits strong versatility in objective function, i.e. it is applicable not only to frequency and displacement responses but also to MAC, stress–strain, neutral axis, and other objective functions. In terms of structural types, this method is also applicable to FEMU for different structures, allowing for the adaptive generation of specific weight coefficient combinations based on experimental data. It provides a systematic and efficient solution to the complex weight-setting problem, especially demonstrating greater convenience and robustness when updating based on multiple response targets. Compared to traditional model updating methods, the FEMU using this framework achieves higher predictive accuracy in key responses. Its applicability will be further validated through the subsequent numerical example and real bridge analysis.

Fig. 1 shows the flowchart for FEMU, incorporating the proposed two-stage adaptive weight coefficients, Kriging model and PSO. The detailed steps are described as follows.

Step 1: Establish the initial FE model based on the design documents.

Step 2: Select parameters to be updated based on local sensitivity analysis, and use Latin Hypercube Design (LHD) to produce parameter sample data. Substitute these parameter samples into the FE model to obtain the corresponding structural response samples.

Step 3: Construct the Kriging model based on the sample data obtained in Step 2, and evaluate the model accuracy using Mean Square Error (MSE). If the accuracy meets the requirements, proceed to Step 4, but if not, return to Step 2 to rebuild the samples.

Step 4: Construct the first-stage adaptive weight objective function based on Eqs. (7) and (8), and utilize the PSO algorithm to perform the first-stage FEMU.

Step 5: Use the first-stage updated model as the initial model for the second stage. Construct the second-stage adaptive weight objective function based on Eqs. (9)–(12), and apply the PSO algorithm for the second stage of model updating.

Step 6: Evaluate the updated FE model by analyzing the relative errors of frequencies and displacements between the updated FE model and experimental measurements.

3. A numerical example

3.1. Simply supported planar truss

This section conducts a numerical simulation on a damaged simply supported planar truss structure under noise conditions to evaluate the effectiveness of the proposed two-stage adaptive weight coefficients, as shown in Fig. 2. Especially, the proposed method's capability to identify the predetermined damage under noise conditions through the dynamic adjustment of weight coefficients is validated. The truss has a height of 1 m and a span of 9 m, with each individual truss segment having a standard span of 1.5 m. All truss members have a cross-sectional area of 1 cm^2, with an initial elastic modulus of 2.31×10^4 MPa and an initial density of 7020 kg/m^3. Concentrated loads of 2 kN and 5 kN are applied at nodes 6 and 8, respectively. To simulate the stiffness and mass reduction caused by structural damage such as cracking and material degradation, the following damage conditions are set. The elastic modulus of the upper chord members (denoted by E_1), web members (denoted by E_2), and lower chord members (denoted by E_3) are reduced by 10 %, 20 %, and 15 %, respectively. The density D is reduced by 10 %. The initial relative errors of the above four parameters in the initial model compared to those in the damaged model are 11.11 %, 25 %, 17.65 %, and 11.11 %, respectively. The parameters' initial values are set to 1 for easy comparison. Therefore, the damage coefficients are 0.9 for E_1, 0.8 for E_2, 0.85 for E_3, and 0.9 for D. The parameter optimization range is set to 0.7 to 1.3 times the initial values. The structural responses involved in numerical simulation include the first six natural frequencies and the vertical displacements at the measurement points 3, 5, 7, 9, and 11, as illustrated in Fig. 2.

3.2. Noise conditions

Different white noise levels were added to the 5th and 6th order frequencies and displacements at points 3 and 11 to simulate measurement errors. The four noise scenarios are: no noise, 3 %, 5 %, and 10 %. Table 1 compares the calculated frequencies and displacements obtained from the initial FE model and damage model under different noise conditions.

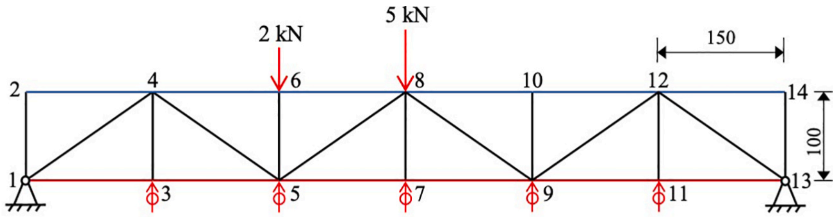

Fig. 2. Planar truss structure (dimensions in cm).

Table 1
Comparison of the calculated structural response values obtained from the initial model and damage model under different noise conditions.

Structural response	Unit	Undamaged (Initial structure)	Damaged ("True" structure)				Relative error (%)
			No noise	3 % noise	5 % noise	10 % noise	Initial vs No noise
f_1	Hz	14.029	13.759	13.759	13.759	13.759	1.96
f_2	Hz	33.468	32.362	32.362	32.362	32.362	3.42
f_3	Hz	59.453	57.526	57.526	57.526	57.526	3.35
f_4	Hz	63.935	61.129	61.129	61.129	61.129	4.59
f_5	Hz	102.470	97.046	99.958	101.899	106.751	5.59
f_6	Hz	112.711	107.883	111.120	113.277	118.671	4.48
d_1	mm	−32.16	−37.08	−38.20	−38.94	−40.79	−13.26
d_2	mm	−69.16	−79.85	−79.85	−79.85	−79.85	−13.38
d_3	mm	−78.17	−90.86	−90.86	−90.86	−90.86	−13.97
d_4	mm	−62.54	−71.98	−71.98	−71.98	−71.98	−13.11
d_5	mm	−27.88	−32.00	−32.96	−33.60	−35.20	−12.88

3.3. Discussion of updating results

The truss model under the four noise conditions was updated using both the equal-weight and the adaptive weight objective functions described in Section 3. The objective function was defined using the residuals of frequencies and displacements, as illustrated by Eq. (6). The PSO's algorithm parameters were set as follows. The population size is 20 and the maximum iteration number is 100. The inertia weight η is linearly decreased to balance optimization capability during early and late iterations, which can be expressed by:

$$\eta(k) = \eta_{start} - (\eta_{start} - \eta_{end}) \times k/T_{\max} \tag{13}$$

where η_{start} and η_{end} denote the inertia weights at the start and the end, set to 0.9 and 0.5, respectively, k denotes the current iteration number and $T_{\max}$ denotes the maximum number of iterations. The society and recognition coefficients are all set as 1.5. The simulation is performed using MATLAB (2019) on a system with an Intel Core i5-10400F processor running at 2.90 GHz and 16 GB of RAM. The statistical results obtained from 200 independent runs are analyzed to avoid the randomness of the PSO.

Fig. 3 shows the weight coefficients of frequencies and displacements in the first stage, which are calculated by Eqs. (7) and (8). It can be observed that the low-order frequencies and large displacements are assigned with high weight coefficients. Fig. 4 shows the variation of the frequency and displacement weight coefficients with iterations in the second stage. It can be observed that the weight coefficients of the first four frequencies and the middle three displacement points, unaffected by noise, gradually increase with iteration until they stabilize. Conversely, the weight coefficients of the 5th and 6th natural frequencies and the 1st and 5th displacements that are affected by noise gradually decrease throughout the iteration process. These results demonstrate that the proposed adaptive weight coefficients successfully identify response data with higher reliability and adjust weight coefficients, thereby reducing the impact of noise on model updating.

Fig. 5 compares the updating parameters among their true values (predetermined damage), and identified the mean values from 200 independent runs by equal weight and adaptive weight coefficients under different noise conditions. The standard deviations of the identified values are also plotted for comparison. Under the zero noise condition, both the equal weight and adaptive weight coefficients identify the predetermined damage. The identified values closely match the damage values with a slight standard deviation. However, as the noise level increases, the identified values obtained from the equal weight objective function gradually deviate from the true values, while those obtained from the adaptive weight coefficients objective function remain consistent with the true values. Additionally, the adaptive weight coefficients objective function performs better than the equal weight one in terms of standard deviation. For instance, under 5 % noise interference, the maximum error in the identified values for the equal weight objective

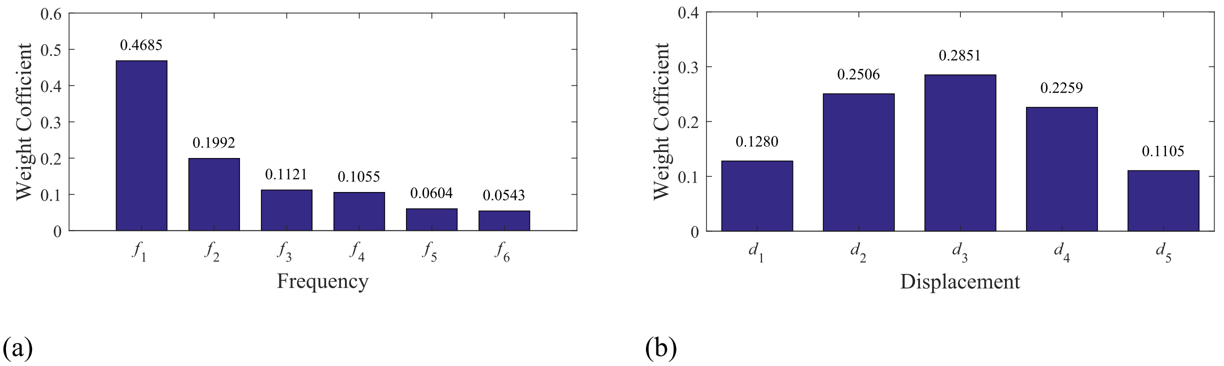

Fig. 3. Weight coefficients in the first stage: (a) Frequency and (b) displacement.

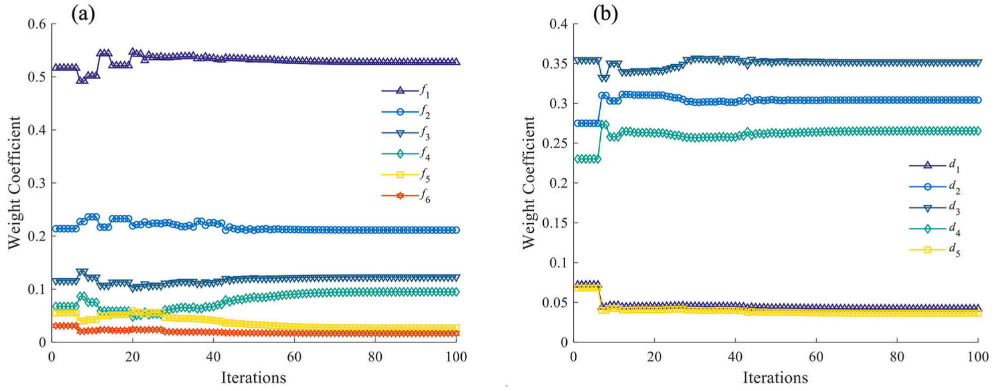

Fig. 4. Variation of weight coefficients with iterations in the second stage: (a) Frequency and (b) displacement.

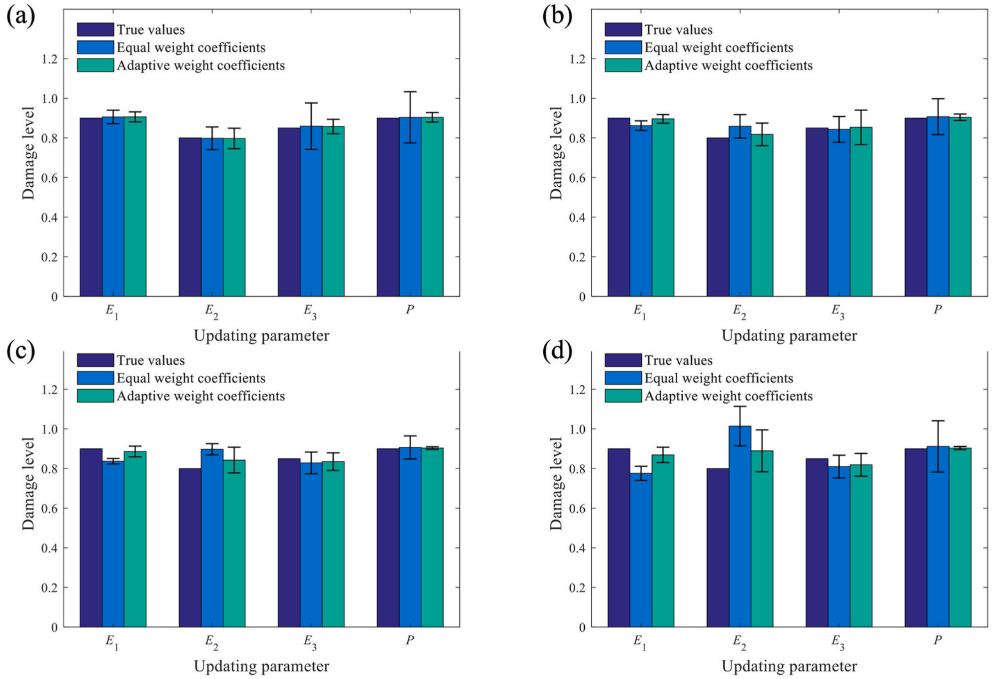

Fig. 5. Comparison of parameters among true values (predetermined damage), identified values by equal weight and adaptive weight coefficients under different noise conditions: (a) 0%, (b) 3%, (c) 5% and (d) 10%.

function is 12.17 %, whereas for the adaptive weight objective function, it is reduced to 5.35 %. Under 10 % noise interference, the maximum standard deviation of the identification values for the equal weight objective function is 0.13, while the maximum standard deviation for the adaptive weight coefficients objective function is only 0.106. These results indicate that the proposed adaptive weight coefficients can provide accurate results under noise conditions and outperforms the equal weight method in terms of identification accuracy and stability.

Fig. 6 compares the frequency and displacement relative errors after model updating with equal weight and adaptive weight coefficients under different noise conditions. It should be noted that the relative errors plotted in Fig. 6 are the mean values obtained from 200 independent runs. Under noise-free conditions, both equal weight and adaptive weight coefficients objective functions accurately predict the response, and the relative errors in frequencies and displacements are all below 0.2 %. As the noise interference increases, the relative errors of frequencies and displacements obtained from the adaptive weight coefficients objective function are smaller than those obtained from the equal-weight objective function. For example, at the 10 % noise level, the maximum errors in frequency and displacement updated by the equal-weight objective function are 10.12 % and 4.55 %, respectively. In comparison, those obtained from the adaptive weight coefficients objective function are 4.82 % and −0.50 %. Overall, the adaptive weight coefficients objective function has resulted in effective updates for both frequencies and displacements. For frequencies, the relative errors of the first three order frequencies are all less than 1 %. Due to errors in the experimental data for the last two frequencies, the adaptive weight

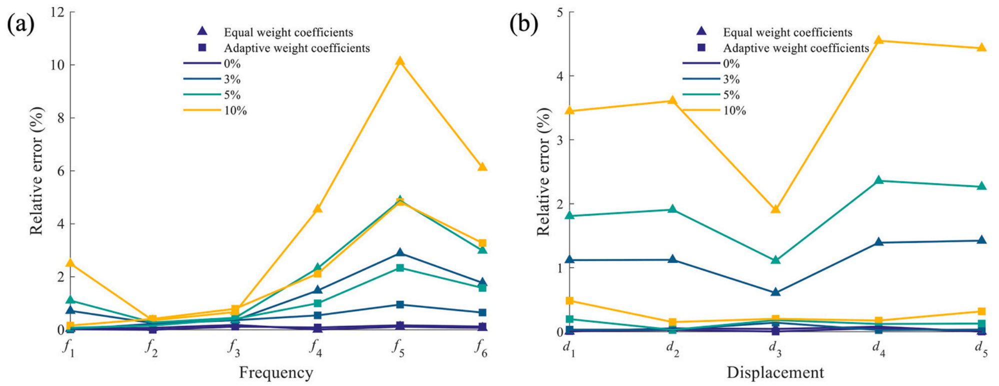

Fig. 6. Comparison of the response relative errors after model updating with equal weight and adaptive weight under different noise conditions: (a) Frequency and (b) displacement.

coefficients automatically reduced the weights, resulting in less effective updates compared to the lower-order frequencies. Nevertheless, the relative errors of the last two frequencies are still below 5 %. For displacements, the relative errors obtained from adaptive weight coefficients are all below 1 %, even under the 10 % noise level. Meanwhile, that obtained from equal weight method reaches up to 4.5 %. These data demonstrate the superior updating performance of the adaptive weight coefficients objective function under noise interference. This is due to the adaptive weighting mechanism, which dynamically optimizes the weight distribution, making the update of key responses more precise and stable, thereby improving the accuracy of the updated FE model in evaluating the structural physical properties. The engineering applicability of this method will be further validated in practical bridge analysis.

4. Model updating of cable-stayed bridge

4.1. Bridge description

The Ganjiang (GJ) Bridge, a long-span cable-stayed bridge, has a span layout of (35 + 40 + 60 + 300 + 60 + 40 + 35) meters. It is

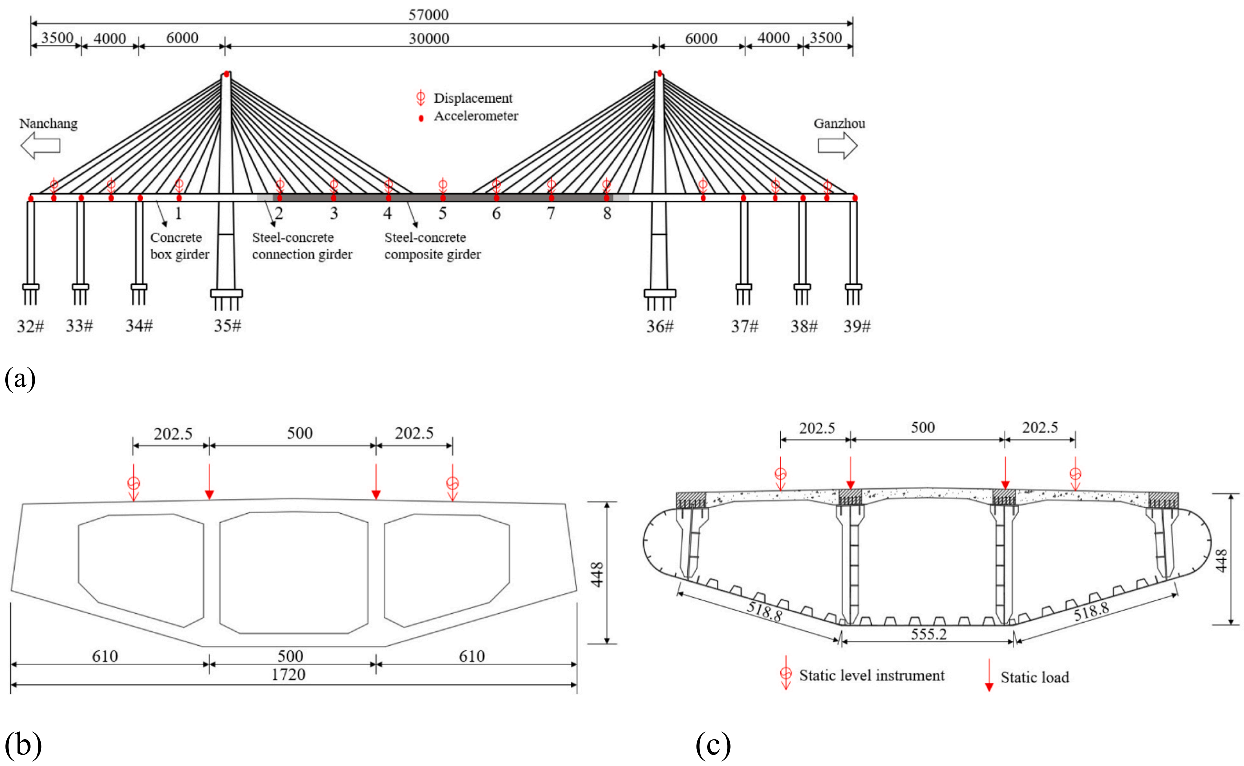

Fig. 7. The GJ Bridge: (a) Configuration of the bridge elevation, (b) concrete box girder and (c) composite girder (dimensions in cm).

designed for high-speed railways with a 350 km/h maximum speed. The main girder consists of a steel–concrete composite girder and a concrete box girder. One side of the concrete main girder is 155.7 m long, while the steel–concrete composite segment is centrally positioned within 20 m of the two cable towers. The bridge towers adopt a large-radius curved A-shaped concrete design. The total heights of towers 35# and 36# above their bases are 124.5 m and 127.6 m, respectively. The stay cables are configured in a fan shape within a spatial double-cable-plane system. The bridge includes 48 pairs of stay cables. The cable spacing is 10. 5 m on the concrete girder, 12 m on the steel–concrete composite girder, and ranges from 1.8 to 3.0 m on the towers. The cable towers are equipped with built-in steel anchor boxes to anchor the stay cables. It is essential to establish an accurate FE model for bridge health monitoring during the operational stage [45]. Fig. 7 illustrates the elevation layout of the GJ Bridge and the arrangement of static and dynamic measurement points.

4.2. The initial FE model

MIDAS Civil 2019 was utilized to establish the bridge's initial FE model. The main girder, main towers, and auxiliary piers were modeled using beam elements. Beam elements can efficiently simulate the bending, shear, and axial deformations of bridges and are widely used in the analysis of large-span bridges. The main girder's composite section was modeled using the double-element method, incorporating a rigid connection between the concrete and steel box girder to simulate shear stud effects. Stay cables were modeled using truss elements that only bear tension, with initial prestressing forces applied to simulate cable forces. Regarding boundary conditions, the bases of the piers and towers were simplified as fixed constraints. The stay cables were connected to the main towers and main girder using master–slave constraints. Similarly, the main girder was connected to the auxiliary piers and main towers using master–slave constraints. Fig. 8 shows the initial FE model of the GJ Bridge.

4.3. Static and dynamic tests

An on-site test was conducted to evaluate whether its static and dynamic performance met the design requirements. The static load test measured the displacement and other static characteristics of the main girder under various static load conditions, and the ambient vibration test evaluated the frequencies and other dynamic characteristics of the bridge. Fig. 7 shows the relevant displacement and acceleration measurement points. The detailed test procedures were described in references [34,35]. This study uses the main girder's displacements under three static loading conditions and the bridge's frequencies under ambient vibration to update the initial FE model. Special attention is paid to comparing the updated results obtained from the proposed adaptive weight coefficients and equal weight method. Table 2 summarizes the measured displacement values (EXP) from the static tests and the calculated values (FEA) from the initial FE model for eight measurement points under three load cases (LC), along with the relative errors. The calculated displacements generally exceed the measured ones, suggesting that the initial FE model may have underestimated the structure's overall stiffness. Excluding the absolute displacement values smaller than 10 mm, the maximum relative displacement errors for the remaining measurement points under each condition are 17.85 %,12.66 %, and 9.67 %, respectively.

4.4. Updating parameters selection

The sensitivity analysis focuses on the following eleven parameters: the elastic modulus and material density of the main span steel–concrete composite beam deck (denoted by E_1, D_1, respectively), concrete side beams (denoted by E_2, D_2, respectively), main towers (denoted by E_3, D_3, respectively), main span steel boxes (denoted by E_4, D_4, respectively), stay cables (denoted by E_5, D_5, respectively), and the elastic modulus (denoted by E_6) of auxiliary piers. The first five natural frequencies and vertical displacements at

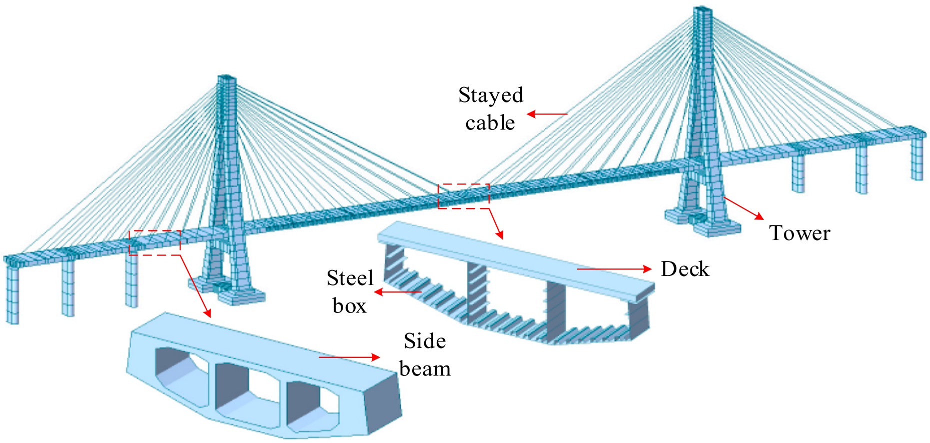

Fig. 8. The initial FE model of the GJ Bridge.

Table 2
Comparison of the experimentally measured displacements (EXP) with the calculated ones from the initial FE model (FEA).

Test point	Load Case 1			Load Case 2			Load Case 3		
	EXP (mm)	FEA (mm)	Error (%)	EXP (mm)	FEA (mm)	Error (%)	EXP (mm)	FEA (mm)	Error (%)
1	4.70	5.53	17.74	11.86	12.25	3.26	11.37	11.19	−1.59
2	−34.37	−40.32	17.31	−71.55	−80.60	12.65	−69.17	−75.86	9.67
3	−73.48	−86.59	17.85	−163.25	−181.79	11.36	−172.26	−186.98	8.54
4	−68.48	−79.21	15.66	−217.77	−242.85	11.52	−251.64	−271.84	8.03
5	−39.92	−44.40	11.22	−188.31	−212.15	12.66	−252.61	−274.98	8.85
6	−15.57	−14.84	−4.72	−103.10	−112.68	9.29	−170.81	−185.19	8.42
7	−3.26	−1.64	−49.79	−37.24	−38.37	3.02	−72.36	−77.46	7.05
8	0.28	0.73	−160.36	−7.85	−8.24	5.01	−17.70	−19.79	11.81

measurement points 1 to 8 under three load cases are selected as structural responses to implement sensitivity analysis. Fig. 9 shows the sensitivities of displacement and frequency. The sensitivity analysis results indicate that E_3, E_4, and E_5 significantly impact the displacements, while D_1, E_2, E_3, D_3, E_4, D_4, and E_5 significantly affect the frequencies. Therefore, the following seven parameters are selected as updating parameters: D_1, E_2, E_3, D_3, E_4, D_4, and E_5.

4.5. Establishment of the Kriging model

LHD [9] was used to generate the sample data of the updating parameters. The design space of elastic modulus E_i was $[0.7E_i, 1.3E_i]$, and that of material density D_i was $[0.8D_i, 1.2D_i]$. The Kriging surrogate models for frequencie**s** and displacements were established using the Matlab toolbox DACE 2.0 created by Lophaven. [46]. Fig. 10**(a)** plots the Kriging model of the first frequency, with its MSE displayed in Fig. 10**(b)**. In Fig. 10**(a)**, the surface represents the predicted values of the Kriging model, and the data points indicate the sample design values used to construct the Kriging surrogate model. It can be observed that the maximum MSE is smaller than 4.0×10^{-10}, indicating that the first natural frequency is predicted with sufficient accuracy. Furthermore, the determination coefficients R^2 of the surrogate model for all structural response exceed 0.99, demonstrating its ability to fit each response with sufficient accuracy.

4.6. Discussions of the results

The objective function is constructed based on the residual functions of calculated and measured displacements and frequencies. The weight values are determined by the equal weight and the proposed adaptive weight coefficients, respectively. The PSO algorithm's parameters are consistent with those described in Section 4. Fig. 11 shows the first-stage weight coefficients determined by the two-stage adaptive weight coefficient. The high weights are assigned to low-order frequencies and large displacements. As introduced in the previous sections, the low-order frequencies of a bridge are easy to excite and usually have high accuracy in operational modal analysis. In terms of displacement, the large displacement values in a load case have a higher contribution to stiffness and bearing capacity evaluation than small displacement values. Additionally, the small displacement values usually have high test errors. A slight variation in small displacement induces high relative error. Fig. 12 shows the variation of the frequency and displacement weight coefficients with the iterations in the second-stage model updating.

As shown in Fig. 12**(a)**, the weight coefficients of the first and third frequencies are increasing, while the second and fifth frequencies are decreasing with iterations. The reason can be attributed to the fact that the second and fifth frequencies have higher relative errors than those of the first and third frequencies. In the second stage, high weights are assigned to the responses with small relative errors. This measure ensures that the response with a small relative error still has high prediction accuracy when the responses

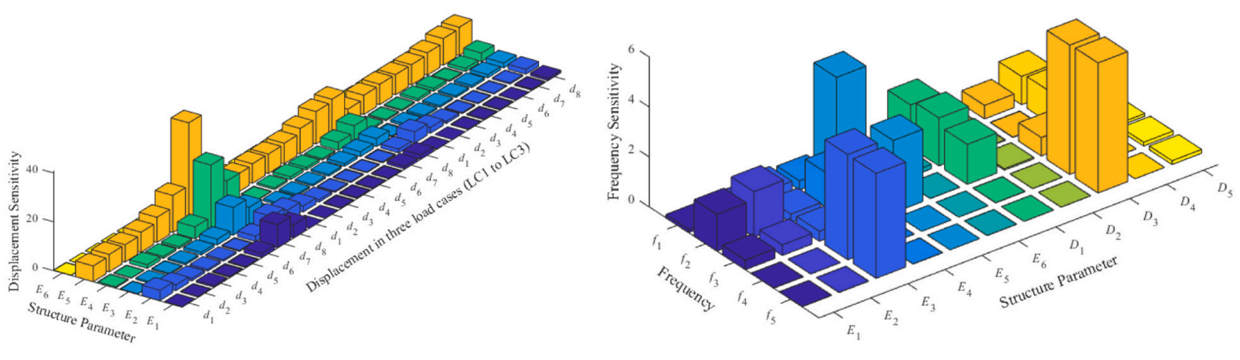

(a) **(b)**

Fig. 9. Sensitivity analysis: (a) Displacement and (b) frequency.

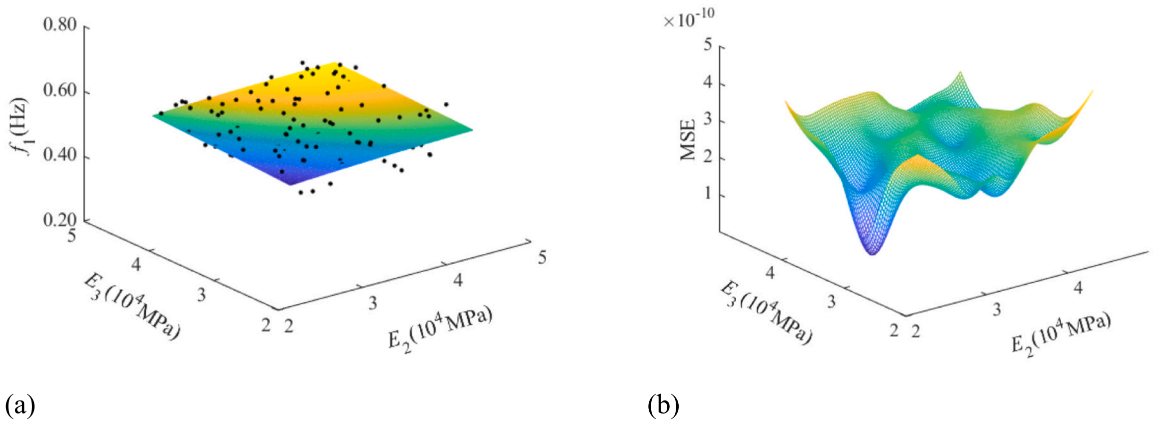

Fig. 10. The Kriging model of the f_1: (a) Kriging response surface and (b) MSE surface.

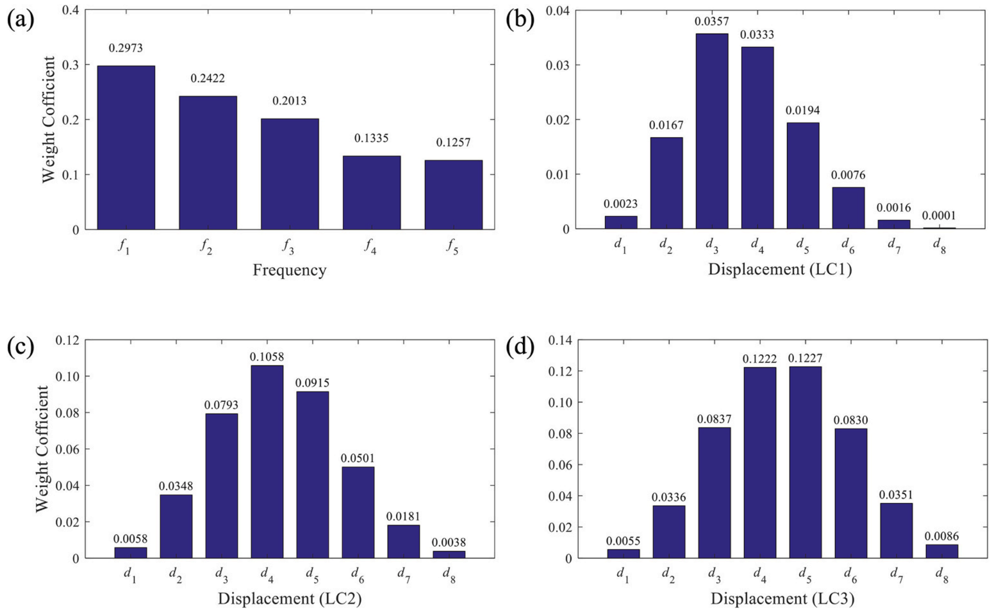

Fig. 11. Weight coefficients in the first stage: (a) Frequency, (b) displacement (LC1), (c) displacement (LC2) and (d) displacement (LC3).

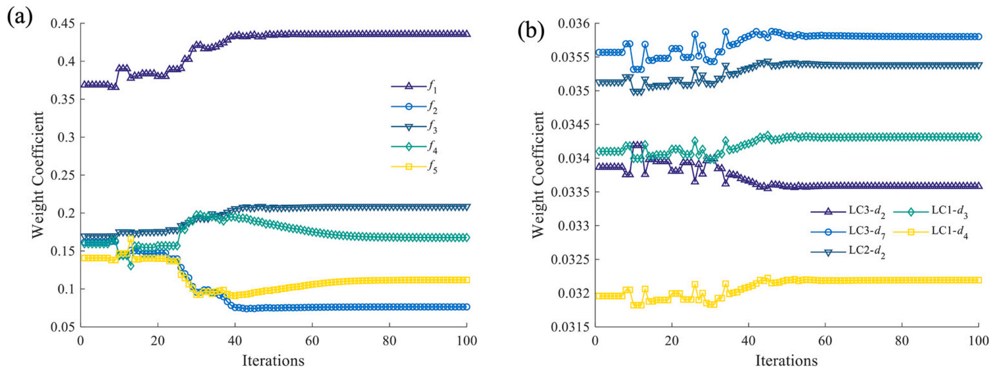

Fig. 12. Variation of weight coefficients with iterations in the second stage: (a) Frequency and (b) displacement.

with high relative errors are effectively updated. Fig. 12**(b)** plots the weight coefficients of the displacement valued at around 70 mm in three load cases. It can be observed that the weight coefficients of displacements have small fluctuations during iteration. These results indicate that relative errors of displacements around 70 mm have similar relative errors. Nevertheless, the performance of the proposed adaptive weight coefficients should be evaluated by analyzing the updated FE model's prediction accuracy.

Table 3 compares the frequencies obtained from the experiment and the initial FE model, as well as the updated values obtained using equal weight and adaptive weight. After the model update, the relative errors of frequencies are significantly reduced. The adaptive weight coefficients provide smaller frequency relative errors than the equal weight method. For example, the relative errors of the fourth and fifth frequencies obtained from equal weight are −12.17 % and −16.98 %, respectively, while those obtained from adaptive weight are 0.23 % and −5.33 %, respectively. These results indicate that the adaptive weight coefficients outperform the equal weight method.

Fig. 13 shows the displacement relative errors predicted by the initial FE model and the updated FE models obtained from equal weight and adaptive weight coefficients. In most cases, the adaptive weight coefficients perform better than the equal weight method, as indicated by the minor relative errors. For instance, at test point 5 under load case 1, the initial relative displacement error is 11.22 %. The updated relative error obtained from equal weight and adaptive weight coefficients is 7.46 % and 3.41 %, respectively. For the displacement at point 6 in LC1 and point 4 in LC3, the equal weight obtained smaller relative errors than the adaptive weight coefficients. The absolute value of the displacement at point 6 in LC1 is only −15.57 mm, which is small. In this case, the adaptive weight coefficients will assign small values during iteration. For the displacement at point 4 in LC3, the relative error obtained from equal weight and adaptive weight coefficients is 0.7 % and 1.45 %, respectively. These data indicate that the two weight methods obtained similar prediction accuracy. Nevertheless, the results presented in Fig. 13 clearly show that the adaptive weight coefficients outperform the equal weight method in terms of displacement prediction accuracy. In summary, the proposed adaptive weight coefficients obtain higher prediction accuracy than the equal weight method regarding frequency and displacement.

5. Conclusions

This paper proposes two-stage adaptive weight coefficients that considers the relative importance and errors of bridge static and dynamic measurements. In the first stage, high weight coefficients are assigned to low-order frequencies and large displacements. In the second stage, the weight coefficients are adaptively adjusted to give high impact to those responses with small relative errors. A FEUM framework is presented based on the proposed two-stage adaptive weight coefficients, Kriging model, and PSO algorithm. The performance of the adaptive weight coefficients is tested through numerical simulation of a damaged truss under various noise conditions and FEUM of a full-scale bridge. The conclusions drawn are as follows.

(1) Compared to the equal weight method, the proposed two-stage weight coefficients can better evaluate the importance of response according to its measurement error and increase the prediction accuracy of the updated FE model. The adaptive weight coefficients obtain better-updating results than the equal weight method in the two case studies.

(2) The damaged simply supported truss under noisy conditions demonstrated that the adaptive weight coefficients can identify the predetermined damage with high accuracy and stability. The noise-affected responses can be identified and automatically assigned with small weight coefficients. With the increase in noise levels, the advantage of the adaptive weight coefficients is significant.

(3) Combined with the updating tool, the proposed adaptive weight coefficients successfully updated the initial FE model of the GJ Bridge. Compared to equal weight method, the adaptive weight coefficients yield smaller response relative errors in most cases. After the model update, the relative errors are around 5 % for frequencies and approximately 10 % for displacements.

(4) Compared to traditional model updating methods that lack standardized protocols and rely on researchers' experience to set weights, the two-stage adaptive weight coefficients updating framework proposed in this study offers greater versatility. In terms of update objectives, this framework is not only applicable to frequency and displacement responses, but can also be extended to other key structural response types that require weight optimization. In terms of structural applications, the method is applicable not only to cable-stayed bridges, but can also be extended to other types of bridges. Furthermore, it holds significant research value for structural model updating problems beyond bridge engineering.

Table 3
Comparison of the frequencies among their experimental values, initial values and updated values obtained from equal weight and adaptive weight coefficients.

Modal order	Frequency (Hz)				Relative error (%)		
	Exp. value	Initial value	Equal weight	Adaptive weight	Initial value	Equal weight	Adaptive weight
1	0.537	0.523	0.542	0.541	−2.61	0.87	0.75
2	0.659	0.570	0.607	0.618	−13.51	−7.82	−6.18
3	0.793	0.782	0.828	0.829	−1.39	4.35	4.48
4	1.196	1.019	1.050	1.199	−14.80	−12.17	0.23
5	1.270	1.022	1.054	1.202	−19.53	−16.98	−5.33

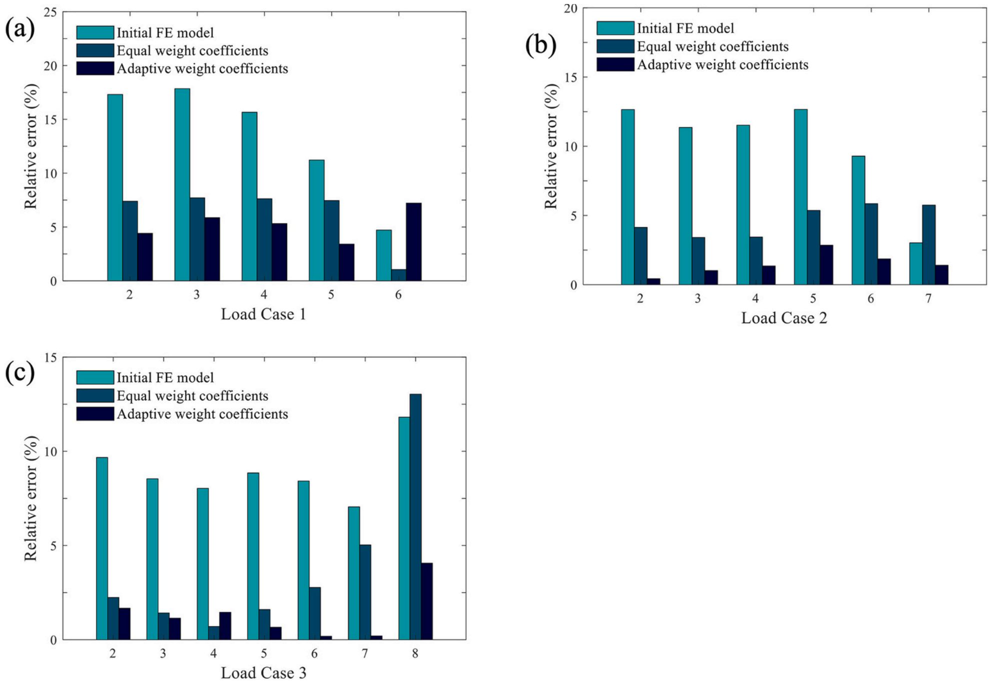

Fig. 13. The relative errors of displacement between initial and updated FE models: (a) LC1, (b) LC2 and (c) LC3.

CRediT authorship contribution statement

Shiqiang Qin: Conceptualization, Investigation, Methodology, Writing – original draft. **Jialong Huang:** Data curation, Investigation, Writing – review & editing. **Shiwei Li:** Data curation, Investigation. **Yunlai Zhou:** Investigation, Methodology. **Magd Abdel Wahab:** Writing – review & editing, Validation, Supervision.

Declaration of competing interest

The authors declare that they have no known competing financial interests or personal relationships that could have appeared to influence the work reported in this paper.

Acknowledgements

This research was financially supported by the Natural Science Foundation of China (Grant No. 51608408), the Fundamental Research Funds for the Central Universities (Grant No.: 2023IV001h), and the Natural Science Basis Research Plan in Shaanxi Province of China (2023-JC-YB-007).

Data availability

Data will be made available on request.

References

[1] N.F. Alkayem, M. Cao, Y. Zhang, et al., Structural damage detection using finite element model updating with evolutionary algorithms: a survey, Neural Comput. Appl. 30 (2018) 389–411.
[2] P. Seventekidis, D. Giagopoulos, Model error effects in supervised damage identification of structures with numerically trained classifiers, Mech. Syst. Sig. Process. 184 (2023) 109741.
[3] H. Gou, Y. He, W. Zhou, et al., Experimental and numerical investigations of the dynamic responses of an asymmetrical arch railway bridge, Proc. Instit. Mech. Eng., Part f: J. Rail Rapid Transit 232 (9) (2018) 2309–2323.
[4] Q. Li, X. Du, P. Ni, et al., Efficient Bayesian inference for finite element model updating with surrogate modeling techniques, J. Civ. Struct. Heal. Monit. (2024) 1–19.
[5] X. Ye, B. Chen, Model updating and variability analysis of modal parameters for super high-rise structure, Concurrency Comput. Pract. Exper. 31 (12) (2019) e4712.
[6] Q. Zhu, Y.L. Xu, X. Xiao, Multiscale modeling and model updating of a cable-stayed bridge. I: Modeling and influence line analysis, J. Bridg. Eng. 20 (10) (2015) 04014112.
[7] H. Gou, T. Zhao, S. Qin, et al., In-situ testing and model updating of a long-span cable-stayed railway bridge with hybrid girders subjected to a running train, Eng. Struct. 253 (2022) 113823.

[8] L. Luo, Y. Xia, A. Wang, et al., Finite element model updating method for continuous girder bridges using monitoring responses and traffic videos, Struct. Control Health Monit. 29 (11) (2022) e3062.
[9] R. Ferrari, D. Froio, E. Rizzi, et al., Model updating of a historic concrete bridge by sensitivity-and global optimization-based Latin Hypercube Sampling, Eng. Struct. 179 (2019) 139–160.
[10] S. Ereiz, I. Duvnjak, J.F. Jiménez-Alonso, Review of finite element model updating methods for structural applications, Structures 41 (2022) 684–723.
[11] E. Samaniego, C. Anitescu, S. Goswami, et al., An energy approach to the solution of partial differential equations in computational mechanics via machine learning: Concepts, implementation and applications, Comput. Methods Appl. Mech. Eng. 362 (2020) 112790.
[12] X. Zhuang, H. Guo, N. Alajlan, et al., Deep autoencoder based energy method for the bending, vibration, and buckling analysis of Kirchhoff plates with transfer learning, Eur. J. Mech.-A/solids 87 (2021) 104225.
[13] A. Osyczka, An approach to multicriterion optimization problems for engineering design, Comput. Methods Appl. Mech. Eng. 15 (3) (1978) 309–333.
[14] O. Cuate, O. Schütze, Pareto explorer for finding the knee for many objective optimization problems, Mathematics 8 (10) (2020) 1651.
[15] S.W. Lin, Y.L. Du, T.H. Yi, et al., Model updating using bridge influence lines based on an adaptive metamodel global optimization method, J. Bridg. Eng. 27 (3) (2022) 04022003.
[16] N.F. Alkayem, M. Cao, Damage identification in three-dimensional structures using single-objective evolutionary algorithms and finite element model updating: evaluation and comparison, Eng. Optim. 50 (10) (2018) 1695–1714.
[17] Ş.Y. Balaman, Investment planning and strategic management of sustainable systems for clean power generation: An ε-constraint based multi objective modelling approach, J. Clean. Prod. 137 (2016) 1179–1190.
[18] X. Xing, Y. Yan, H. Zhang, et al., Optimal design of distributed energy systems for industrial parks under gas shortage based on augmented ε-constraint method, J. Clean. Prod. 218 (2019) 782–795.
[19] J. Lin, Multiple-objective problems: Pareto-optimal solutions by method of proper equality constraints, IEEE Trans. Autom. Control 21 (5) (1976) 641–650.
[20] K. Christodoulou, E. Ntotsios, C. Papadimitriou, et al., Structural model updating and prediction variability using Pareto optimal models, Comput. Methods Appl. Mech. Eng. 198 (1) (2008) 138–149.
[21] S. Ereiz, J.F. Jiménez-Alonso, C. Gallegos-Calderón, et al., Vibration based single-objective finite element model updating using cooperative game theory approach, Mech. Syst. Sig. Process. 212 (2024) 111316.
[22] J.F. Jimenez-Alonso, J. Naranjo-Perez, A. Pavic, et al., Maximum likelihood finite-element model updating of civil engineering structures using nature-inspired computational algorithms, Struct. Eng. Int. 31 (3) (2021) 326–338.
[23] S. Kim, N. Kim, Y.S. Park, et al., A sequential framework for improving identifiability of FE model updating using static and dynamic data, Sensors 19 (23) (2019) 5099.
[24] M.I. Friswell, J.E. Mottershead, Finite Element Model Updating in Structural Dynamics, Kluwer Academic Publishers, 1995.
[25] S.S. Jin, S. Cho, H.J. Jung, et al., A new multi-objective approach to finite element model updating, J. Sound Vib. 333 (11) (2014) 2323–2338.
[26] C. Cismaşiu, A.C. Narciso, F.P. Amarante dos Santos, Experimental dynamic characterization and finite-element updating of a footbridge structure, J. Perform. Constr. Facil 29 (4) (2015) 04014116.
[27] H. Li, H. Ding, Reduction-based model updating of a scaled offshore platform structure, J. Eng. Mech. 136 (2) (2010) 131–142.
[28] L. Deng, C.S. Cai, Bridge model updating using response surface method and genetic algorithm, J. Bridg. Eng. 15 (5) (2010) 553–564.
[29] L. He, E. Reynders, J.H. García-Palacios, et al., Wireless-based identification and model updating of a skewed highway bridge for structural health monitoring, Appl. Sci. 10 (7) (2020) 2347.
[30] E.L. Eskew, S. Jang, Remaining stiffness estimation of buildings using incomplete measurements, Struct. Control Health Monit. 24 (4) (2017) e1899.
[31] S. Ye, X. Lai, I. Bartoli, et al., Technology for condition and performance evaluation of highway bridges, J. Civ. Struct. Heal. Monit. 10 (2020) 573–594.
[32] S.W. Doebling, C.R. Farrar, Computation of structural flexibility for bridge health monitoring using ambient modal data, 1996.
[33] B. Jaishi, H.J. Kim, M.K. Kim, et al., Finite element model updating of concrete-filled steel tubular arch bridge under operational condition using modal flexibility, Mech. Syst. Sig. Process. 21 (6) (2007) 2406–2426.
[34] S. Qin, Y. Yuan, S. Han, et al., A novel multiobjective function for finite-element model updating of a long-span cable-stayed bridge using in situ static and dynamic measurements, J. Bridg. Eng. 28 (1) (2023) 04022131.
[35] S. Qin, S. Han, S. Li, In-situ testing and finite element model updating of a long-span cable-stayed bridge with ballastless track, Structures. 45 (2022) 1412–1423.
[36] J.B. Liao, G.W. Tang, F. Pan, Finite element model updating of existing T-Girder bridge by field quasi-static generalized influence line, Appl. Mech. Mater. 226 (2012) 1609–1613.
[37] R.J. Allemang, The modal assurance criterion - Twenty years of use and abuse, J. Sound Vib. 37 (8) (2003) 14–23.
[38] A.I.J. Forrester, A.J. Keane, Recent advances in surrogate-based optimization, Prog. Aerosp. Sci. 45 (1–3) (2009) 50–79.
[39] J. Søndergaard, Optimization using surrogate models-by the Space, Mapping Technique. (2003).
[40] J.T. Wang, C.J. Wang, J.P. Zhao, Frequency response function-based model updating using Kriging model, Mech. Syst. Sig. Process. 87 (2017) 218–228.
[41] D.R. Jones, M. Schonlau, W.J. Welch, Efficient global optimization of expensive black-box functions, J. Glob. Optim. 13 (1998) 455–492.
[42] J. Kennedy, R. Eberhart, Particle swarm optimization, in: Proceedings of ICNN'95-international conference on neural networks. ieee, 1995, 4: 1942-1948.
[43] A.V. Vasileva, A.S. Vasilev, I.A. Konyakhin, Vision-based system for long-term remote monitoring of large civil engineering structures: design, testing, evaluation, Meas. Sci. Technol. 29 (11) (2018) 115003.
[44] M. Ostrowski, B. Blachowski, B. Wójcik, et al., A framework for computer vision-based health monitoring of a truss structure subjected to unknown excitations, Earthq. Eng. Eng. Vib. 22 (1) (2023) 1–17.
[45] X. Sheng, W. Zheng, Z. Zhu, et al., Ganjiang Bridge: a high-speed railway long-span cable-stayed bridge laying ballastless tracks, Struct. Eng. Int. 31 (1) (2021) 40–44.
[46] S.N. Lophaven, H.B. Nielsen, J. Søndergaard, DACE: a Matlab kriging toolbox. Lyngby, Denmark: IMM, Informatics and Mathematical Modelling, The Technical University of Denmark, 2002.